

Simultaneously Transmitting and Reflecting Reconfigurable Intelligent Surfaces Empowered Cooperative Rate Splitting with User Relaying

Kangchun Zhao, Yijie Mao, *Member, IEEE*, Yuanming Shi *Senior Member, IEEE*

Abstract—In this work, we unveil the advantages of synergizing cooperative rate splitting (CRS) with user relaying and simultaneously transmitting and reflecting reconfigurable intelligent surface (STAR RIS). Specifically, we propose a novel STAR RIS-assisted CRS transmission framework, featuring six unique transmission modes that leverage various combination of the relaying protocols (including full duplex-FD and half duplex-HD) and the STAR RIS configuration protocols (including energy splitting-ES, mode switching-MS, and time splitting-TS). With the objective of maximizing the minimum user rate, we then propose a unified successive convex approximation (SCA)-based alternative optimization (AO) algorithm to jointly optimize the transmit active beamforming, common rate allocation, STAR RIS passive beamforming, as well as time allocation (for HD or TS protocols) subject to the transmit power constraint at the base station (BS) and the law of energy conservation at the STAR RIS. To alleviate the computational burden, we further propose a low-complexity algorithm that incorporates a closed-form passive beamforming design. Numerical results show that our proposed framework significantly enhances user fairness compared with conventional CRS schemes without STAR RIS or other STAR RIS empowered multiple access schemes. Moreover, the proposed low-complexity algorithm dramatically reduces the computational complexity while achieving very close performance to the AO method.

Index Terms—Cooperative rate splitting (CRS), simultaneously transmitting reconfigurable intelligent surface (STAR RIS), rate splitting multiple access (RSMA), max-min fairness (MMF).

I. INTRODUCTION

In sixth-generation (6G) and beyond mobile communications, an increasing number of devices are connecting to the wireless network, causing the following problems: 1) Multi-device connections introduce significant multi-user interference, severely degrading system performance. 2) Ensuring a favorable communication environment for each user becomes highly challenging due to the vast number of devices accessing to the transmission network. To deal these problems, a novel non-orthogonal interference management strategy in the physical (PHY) layer named rate-splitting multiple access (RSMA) comes into our sight. It emerges as a promising technique for enhancing the spectral efficiency and user fairness [2]. RSMA follows the design principle where user messages

are divided into common and private parts at the transmitter. The common parts are encoded into common streams and decoded by multiple users. Meanwhile, the private parts are independently encoded into private streams and decoded only by the corresponding users, following the decoding of the common streams and their subsequent removal through successive interference cancellation (SIC). This empowers RSMA to partially treat interference as noise and partially decode interference. It encompasses various multiple access (MA) schemes like space division MA (SDMA), which fully treats interference as noise, and non-orthogonal MA (NOMA), which fully decodes interference, treating them as special cases [3]–[5].

However, as the common streams of RSMA are required to be decoded by multiple users, the achievable rate will be limited by the user with the weakest channel strength. To overcome this limitation, a novel RSMA scheme named cooperative rate splitting (CRS) is proposed in [6], [7]. This scheme empowers users with stronger channel conditions, acting as relaying users, to transmit the decoded common stream to users with weaker channel conditions. CRS thereby boosts the received signal strengths at the weaker users and improves the achievable common rate. It not only enhances spectral efficiency but also extends radio coverage, promotes user fairness, and reduces energy consumption [7], [8]. There are two transmission phases in CRS, one is the direct transmission phase that the base station (BS) transmits signals to all users, the other is the cooperative transmission phase that the relaying users transmit the decoded common streams to the destination users. According to whether these two phases are executed at the same time, there are two protocols in CRS: *half duplex (HD)* [7] and *full duplex (FD)* [9]. In the HD protocol, the direct and cooperative transmission phases are executed in different time slots, while in the FD protocol, these two transmission phases are executed at the same time. Both protocols demonstrate significant potential in realizing the aforementioned advantages of CRS.

In parallel, reconfigurable intelligent surface (RIS), gaining increasing attention recently, has been viewed as a promising technique in future wireless networks [10]–[12]. A RIS is a two-dimensional (2D) meta-surface containing numerous passive and low-cost reflecting elements which enable to tune the phase shift of the incident signal. By employing the RIS, the line-of-sight (LoS) channel between the BS and users can be reconfigured, effectively improving the spectral efficiency, energy efficiency and extending the communication coverage. Nevertheless, conventional RIS can solely reflect signals, limiting its coverage to a 180° area. This has motivated

A preliminary version of this paper was presented at the IEEE 98th Vehicular Technology Conference, VTC2023-Fall, 2023 [1].

This work has been supported in part by the National Nature Science Foundation of China under Grant 62201347; and in part by Shanghai Sailing Program under Grant 22YF1428400.

K. Zhao, Y. Mao, and Y. Shi are with the School of Information Science and Technology, ShanghaiTech University, Shanghai 201210, China (e-mail: zhaokch12022@shanghaitech.edu.cn, maoyj@shanghaitech.edu.cn, shiym@shanghaitech.edu.cn).

the emergence of a novel RIS that enables to reflect and transmit the incident signal at the same time, which is called simultaneously transmitting and reflecting RIS (STAR RIS) [13] or intelligent omni-surface (IOS) [14]. According to different operating methods, STAR RIS has three protocols: *energy splitting (ES)*, *mode switching (MS)*, and *time switching (TS)*. In the ES protocol, all elements can reflect and transmit the incident signal at the same time. In the MS protocol, each element either reflects or transmits the incident signal. In the TS protocol, the transmission time is split into two time slots. One is the reflection time slot, all elements reflect the incident signal, the other is the transmission time slot, all elements transmit the incident signal. By adjusting the amplitude and phase shift of the reflected and transmitted signals, all three protocols of STAR RIS offer full spatial coverage and additional degrees of freedom (DoF) for the system.

In view of the advantages of the STAR RIS, many existing works have explored its integration with various MA schemes [15]–[20]. In [15], the authors investigated the coverage range of a two-user STAR RIS-aided orthogonal MA (OMA) or NOMA system. In [16], the beamforming optimization was studied in a uplink STAR RIS-aided NOMA system for outage probability minimization and secrecy capacity maximization. In [17], the sum rate maximization was investigated in a downlink STAR RIS-aided NOMA system, wherein the decoding order and transmit beamforming are jointly optimized. Besides, the integration of STAR RIS and RSMA has recently been investigated in some existing works [18]–[20]. In [18], the primary focus was on maximizing the sum secrecy rate in a STAR RIS-aided simultaneous wireless information and power transfer (SWIPT) system using RSMA. In [19], the sum-rate maximization problem for a STAR RIS-aided uplink RSMA system is studied. In [20], efforts were directed towards minimizing the outage probability while considering the spatial correlation among the STAR RIS channels. However, so far, the integration of STAR RIS and CRS has not been investigated yet. And the performance of max-min fairness for STAR RIS-aided RSMA remains unexplored.

Considering the aforementioned advantages of both CRS and STAR RIS, along with the identified research gaps in current literature, there is a compelling incentive to integrate these two techniques. On one hand, the CRS transmission scheme provides robust and flexible interference management to enhance the performance of STAR RIS. On the other hand, STAR RIS reconfigures and improves wireless channels, thereby further enhancing the performance of CRS. Their integration can lead to a mutually beneficial solution. In this work, we delve into the STAR RIS-aided CRS system, and the main contributions of this paper are summarized as follows:

- We propose a novel downlink STAR RIS-aided CRS transmission framework, empowering a STAR RIS to assist both the direct and cooperative transmission phases of CRS. Within this framework, we investigate six different transmission modes including various combinations of CRS relaying protocols (HD and FD) and STAR RIS operating protocols (ES, MS, and TS).
- We formulate a new resource allocation problem with

the objective of maximizing the minimum user rate. To solve this problem, the STAR RIS passive beamforming, the BS active beamforming, common rate allocation, and time slot allocation (in HD or TS protocols) are jointly optimized under the transmit power constraint at the BS and the energy conservation constraints at the STAR RIS. Due to the non-convexity of the formulated problem, we propose an alternative optimization (AO) algorithm to solve the problem. This approach involves decomposing the original problem into two subproblems: the STAR RIS passive beamforming optimization and transmit active beamforming optimization. Each subproblem is then solved using a successive convex approximation (SCA)-based method. Through iterative solving of the two subproblems, we attain a near-optimal solution until convergence.

- We further propose a low-complexity algorithm to solve the formulated problem. For the passive beamforming design, we derive a closed-form solution for the STAR RIS passive beamforming based on the gradient descent approach. To ensure the derived solution meets the STAR RIS constraints, we further use the symmetric unitary projection based on singular value decomposition (SVD) to project the solution into the feasible set of the constraints. For transmit active beamforming, we use the zero-forcing (ZF) approach to fix the beamforming direction. Subsequently, we simply optimize the power allocation using SCA.
- We evaluate the performance of the proposed STAR RIS-aided CRS framework and show the effectiveness of our proposed algorithms by numerical results. Our analysis reveals that the STAR RIS-aided CRS scheme outperforms other STAR RIS-aided MA schemes. We also offer insights into the preferred regions for the six proposed transmission protocols. Moreover, the results demonstrate that our proposed low-complexity algorithm achieves comparable performance while significantly reducing CPU time compared to the AO algorithm.

Organization: The subsequent sections of the paper are organized as follows. Section II delineates the system model and formulates the max-min fairness problem. Section III details the AO optimization framework for the problem and the proposed low-complexity algorithm. Section IV presents numerical results. And Section V concludes the paper.

II. SYSTEM MODEL AND PROBLEM FORMULATION

As illustrated in Fig. 1, we consider a STAR RIS-aided multi-user multiple-input single-output (MISO) downlink transmission network, with CRS supported during the transmission. There is a BS equipped with L transmit antennas, a STAR RIS containing N elements indexed by the set $\mathcal{N} = \{1, \dots, N\}$, and K users indexed by the set $\mathcal{K} = \{1, 2, \dots, K\}$. Each user is equipped with a single transmit antenna and a receive antenna. Given the ability of the STAR RIS to transmit and reflect the incident signal simultaneously, we divide the transmission space into two distinct subspaces, namely, the reflection space and the transmission space. Users

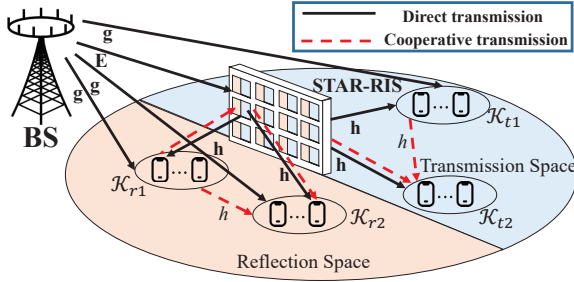


Fig. 1. The transmission architecture of the proposed STAR RIS-assisted CRS.

in the reflection space receive signals reflected by the STAR RIS and are indexed by the set \mathcal{K}_r . Conversely, users in the transmission space receive signals transmitted by the STAR RIS and are indexed by the set \mathcal{K}_t . The two user sets satisfy $\mathcal{K}_r \cup \mathcal{K}_t = \mathcal{K}$ and $\mathcal{K}_r \cap \mathcal{K}_t = \emptyset$. Both subspaces allow user relaying, which further divides the users in each subspace into two user groups: the relaying user group \mathcal{K}_{i1} and the destination user group \mathcal{K}_{i2} , $i \in \{r, t\}$. The user groups satisfy $\mathcal{K}_{r1} \cap \mathcal{K}_{r2} = \emptyset$, $\mathcal{K}_{t1} \cap \mathcal{K}_{t2} = \emptyset$, $\mathcal{K}_{r1} \cup \mathcal{K}_{r2} = \mathcal{K}_r$, and $\mathcal{K}_{t1} \cup \mathcal{K}_{t2} = \mathcal{K}_t$. For simplicity, we denote the relaying user set and the destination user set in the full space as $\mathcal{K}_1 = \mathcal{K}_{t1} \cup \mathcal{K}_{r1}$ and $\mathcal{K}_2 = \mathcal{K}_{t2} \cup \mathcal{K}_{r2}$, respectively. Without loss of generality, we assume users in \mathcal{K}_1 have better channel conditions than users in \mathcal{K}_2 .

In this work, we consider a block-fading channel model with T transmission blocks indexed by the set $\mathcal{T} = \{1, \dots, T\}$. The channels between the BS and STAR RIS, the BS and user- k , STAR RIS and user- k are respectively denoted by $\mathbf{E}(t) \in \mathbb{C}^{N \times L}$, $\mathbf{g}_k(t) \in \mathbb{C}^{L \times 1}$, $\mathbf{h}_k(t) \in \mathbb{C}^{N \times 1}$, where t denotes the t -th block, $t \in \mathcal{T}$. Besides, the channel between user- i to user- j is denoted by $h_{i,j}$. As the pioneer study on STAR RIS-empowered CRS, we employ a simplified CSI model by assuming perfect knowledge of CSI at the BS for all communication links, i.e., perfect CSIT at the transmitter (CSIT). The imperfect CSIT setting can be easily extended based on the existing works on RSMA with imperfect CSIT. It's important to highlight that our primary emphasis is on exploring the diverse performance achieved by various transmission modes of STAR RIS-empowered CRS.

A. Transmission Modes of STAR RIS-empowered CRS

CRS involves two transmission phases: the direct transmission phase and the cooperative transmission phase. During the direct transmission phase, the BS sends signals to all users. In the cooperative transmission phase, users in \mathcal{K}_1 act as relaying users to transmit the decoded common stream to users in \mathcal{K}_2 , utilizing either the HD or FD protocols. The FD protocol allows simultaneous transmission and reception for relaying users. However, this approach introduces self-interference at the relaying users. In the *HD protocol*, each time block is divided into two consecutive parts respectively for the two transmission phases. Let λ ($0 < \lambda \leq 1$) denote the fraction of time allocated to the direct transmission phase, and $(1 - \lambda)$ is the fraction allocated to the cooperative transmission phase.

In this paper, both transmission phases of CRS are assisted by the STAR RIS. According to the principle of single

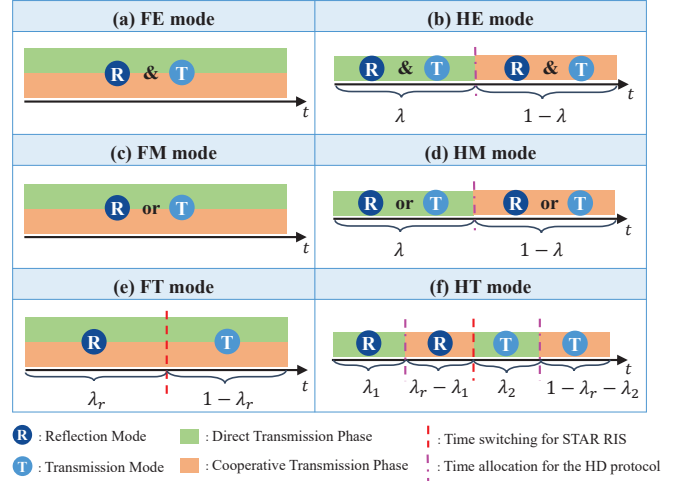


Fig. 2. Six transmission modes of the proposed STAR RIS-assisted CRS.

connected STAR RIS in [13], each element of STAR RIS can operate in the reflection mode and/or the transmission mode according to different operating protocols [13]. The reflection and transmission matrices are all diagonal matrices, denoted as $\Theta_i = \text{diag}(\sqrt{\beta_{1,i}}e^{j\theta_{1,i}}, \dots, \sqrt{\beta_{N,i}}e^{j\theta_{N,i}})$, $i \in \{r, t\}$. In the *ES protocol*, each element of STAR RIS simultaneously reflects and transmits the incident signal. Hence, $\beta_{n,r}$ and $\beta_{n,t}$ should satisfy $\beta_{n,r} + \beta_{n,t} = 1$ and $\beta_{n,r}, \beta_{n,t} \in [0, 1]$. The *MS protocol* is a special case of ES where each element operates in either reflection or transmission mode, resulting in binary values for the amplitude coefficients, i.e., $\beta_{n,r}, \beta_{n,t} \in \{0, 1\}$. In the *TS protocol*, each element of STAR RIS switches between the transmission and reflection modes in each transmission block. Define $0 \leq \lambda_r \leq 1$ as the percentage of time allocated to the reflection mode in each transmission block, $(1 - \lambda_r)$ as the percentage of time allocated to the transmission mode. The TS protocol focuses on designing λ_r and the phase shifts, where $\beta_{n,r} = 1, \beta_{n,t} = 0$ during the λ_r percentage of time and $\beta_{n,r} = 0, \beta_{n,t} = 1$ for the remaining $(1 - \lambda_r)$.

In the proposed STAR RIS-assisted CRS transmission framework, we pair the aforementioned relaying protocols (HD and FD) with the three STAR RIS operating protocols (ES, MS, and TS), yielding six distinct transmission modes for STAR RIS-assisted CRS. These modes are summarized in Fig. 2 and explained as follows:

- *FD-ES (FE) mode*: This refers to the use of the HD protocol for CRS and the ES protocol for the STAR RIS. As illustrated in Fig. 2(a), FE enables each element of the STAR RIS to operate in both transmission and reflection modes simultaneously in the non-orthogonal direct and cooperative transmission phases.
- *HD-ES (HE) mode*: This refers to the use of the HD protocol for CRS and the ES protocol for the STAR RIS. As illustrated in Fig. 2(b), HE enables each element of the STAR RIS to operate in both transmission and reflection modes simultaneously in the orthogonal direct and cooperative transmission phases.
- *FD-MS (FM) mode*: This refers to the use of the FD protocol for CRS and the MS protocol for the STAR RIS. As illustrated in Fig. 2(c), FM enables each element of

the STAR RIS to operate in either transmission or reflection mode in the non-orthogonal direct and cooperative transmission phases.

- *HD-MS (HM) mode*: This refers to the use of the HD protocol for CRS and the MS protocol for the STAR RIS. As illustrated in Fig. 2(d), HM enables each element of the STAR RIS to operate in either transmission or reflection mode in the orthogonal direct and cooperative transmission phases.
- *FD-TS (FT) mode*: This refers to the use of the FD protocol for CRS and the TS protocol for the STAR RIS. As illustrated in Fig. 2(e), each transmission block is split into two time slots based on λ_r ($0 \leq \lambda_r \leq 1$). FT facilitates all elements of the STAR RIS to function in the reflection mode during the initial portion λ_r of the time, while they operate in the transmission mode during the subsequent portion $1 - \lambda_r$ of the time, across the non-orthogonal direct and cooperative transmission phases.
- *HD-TS (HT) mode*: This refers to the use of the HD protocol for CRS and the TS protocol for the STAR RIS. As illustrated in Fig. 2(f), each transmission block is split into two time slots based on λ_r : one for the reflection mode and the other for the transmission mode of STAR RIS. Then, each time slot is further split into two orthogonal parts for the direct and cooperative transmission phases of CRS, resulting in a total of four orthogonal transmission slots. Here, we introduce λ_1 ($0 < \lambda_1 \leq \lambda_r$) and λ_2 ($0 < \lambda_2 \leq 1 - \lambda_r$) to represent the time allocation between the two transmission phases in the reflection and transmission modes, respectively.

Hereinafter, we use j to represent the selected transmission mode, where $j \in \{\text{FE, FM, FT, HE, HM, HT}\}$.

B. Transmit Signal Model

For all six transmission modes described in the previous subsection, the primary differences among them lie in the received signals and the approaches employed to process the received signals. The transmit signals in both the direct and cooperative transmission phases remain consistent, as specified in this subsection.

1) *Direct transmission phase*: We denote W_k as the message intended to user- k . At the BS, according to the principle of 1-layer RSMA [21], [22], W_k is split into a common sub-message $W_{c,k}$ and a private sub-message $W_{p,k}$. All common sub-messages $W_{c,1}, \dots, W_{c,K}$ are collected and then encoded into a common stream s_0 , which is required to be decoded by all users. The individual private sub-message $W_{p,k}$ is independently encoded into a private stream s_k , which is required to be decoded by user- k only. Denote $\mathbf{s} = [s_0, s_1, \dots, s_K]^T$ and $\mathbf{P} = [\mathbf{p}_0, \mathbf{p}_1, \dots, \mathbf{p}_K] \in \mathbb{C}^{L \times (K+1)}$ respectively as the stream vector and the transmit beamforming matrix, where $\mathbf{p}_k \in \mathbb{C}^{L \times 1}$. The transmit signal at the BS in the direct transmission phase is given by

$$\mathbf{x}^{[1]} = \mathbf{P}\mathbf{s} = \sum_{k=0}^K \mathbf{p}_k s_k, \quad (1)$$

where the superscript [1] denotes the direct transmission phase. Here, assuming $\mathbb{E}\{\mathbf{s}\mathbf{s}^H\} = \mathbf{I}$, the transmit power of the BS is

limited by $\text{tr}(\mathbf{P}\mathbf{P}^H) \leq P_t$, where P_t is the maximum transmit power at the BS.

2) *Cooperative transmission phase*: Users in \mathcal{K}_1 employ the decode-and-forward (DF) protocol to decode, re-encode, and subsequently transmit the decoded s_0 to users in \mathcal{K}_2 . The transmit signal at the relaying user- k in the cooperative transmission phase is

$$x_k^{[2]} = \sqrt{P_k} s_0, \quad (2)$$

where the superscript [2] denotes the cooperative transmission phase and P_k is the relaying transmit power at user- k .

C. Received Signal Model for FD-based Transmission Modes

In the FD-based transmission modes (FE, FM, and FT), both the direct and cooperative transmission phases share the same radio resources. Self-interference is inevitably among the relaying users in \mathcal{K}_1 as they simultaneously receive signals from the BS and transmit the common stream s_0 to users in \mathcal{K}_2 , [23], [24]. We denote the self-interference channel as $I_k(t)$, which follows the same distribution $I_k(t) \sim \mathcal{CN}(0, \Omega_I^2)$ for all $k \in \mathcal{K}_1$. The signal received by users in \mathcal{K}_2 from \mathcal{K}_1 , denoted as $\hat{s}_0(t)$, is a delayed version of s_0 , where $\hat{s}_0(t) = s_0(t - t_d)$. Here, t_d represents the processing time for users in \mathcal{K}_1 to decode and forward s_0 . To ensure that the relaying users transmit and receive $\hat{s}_0(t)$ within the same block, we assume that t_d is much smaller than one block period [24], [25]. In this work, we focus on optimizing \mathbf{P} , Θ_r and Θ_t in each transmission block. Hence, we omit t in the following. Next, we will specify the received signals and achievable rates for FE, FM, and FT, respectively.

1) *FE/FM*: When $j = \text{FE}$ or $j = \text{FM}$, the signal received at each relaying user- k in \mathcal{K}_1 is given by

$$y_k^j = \underbrace{\left(\mathbf{g}_k^H + \mathbf{h}_k^H \Theta_i \mathbf{E} \right)}_{\tilde{\mathbf{g}}_{k,i}^H} \mathbf{x}^{[1]} + I_k \sqrt{P_k} \hat{s}_0 + n_k, i \in \{r, t\}, \quad (3)$$

where n_k is the additive white Gaussian noise (AWGN) which follows $n_k \sim \mathcal{CN}(0, \sigma^2)$ and $I_k \sqrt{P_k} \hat{s}_0$ is the self-interference suffered at user- k . Each user- k in \mathcal{K}_1 sequentially decodes the common stream s_0 and the private stream s_k with the assistance of SIC. Let $\tilde{\mathbf{g}}_{k,i}$ denote the effective channel between the BS and user- k , the SINRs of decoding s_0 and s_k at user- k in \mathcal{K}_1 are respectively given as

$$\gamma_{c,k}^{\text{FD}} = \gamma_{c,k}^{\text{FD},[1]} = \frac{|\tilde{\mathbf{g}}_{k,i}^H \mathbf{p}_0|^2}{\sum_{m \in \mathcal{K}} |\tilde{\mathbf{g}}_{k,i}^H \mathbf{p}_m|^2 + |I_k|^2 P_k + \sigma^2}, \quad (4)$$

$$\gamma_k^{\text{FD}} = \frac{|\tilde{\mathbf{g}}_{k,i}^H \mathbf{p}_k|^2}{\sum_{m \in \mathcal{K}, m \neq k} |\tilde{\mathbf{g}}_{k,i}^H \mathbf{p}_m|^2 + |I_k|^2 P_k + \sigma^2}. \quad (5)$$

Each user- k in \mathcal{K}_2 receives signals from both the BS and the relaying users in \mathcal{K}_1 , which is given as

$$y_k^j = \tilde{\mathbf{g}}_{k,i}^H \mathbf{x}^{[1]} + \sum_{m \in \mathcal{K}_1} \underbrace{\left(h_{m,k} + \mathbf{h}_k^H \Theta_i^H \mathbf{h}_m \right)}_{\tilde{h}_{m,k,i}} x_m^{[2]} + n_k, \quad (6)$$

$i \in \{r, t\}$.

Each user in \mathcal{K}_2 then employs the maximal ratio combining (MRC) approach to ensure the received signals are properly co-phased and merged [26]. Denote the effective channel between user- m and user- n as $\tilde{h}_{m,n,i}$, the SINRs of decoding the s_0 and s_k at user- k in \mathcal{K}_2 are given as

$$\gamma_{c,k}^{\text{FD}} = \frac{|\tilde{\mathbf{g}}_{k,i}^H \mathbf{p}_0|^2}{\underbrace{\sum_{m \in \mathcal{K}} |\tilde{\mathbf{g}}_{k,i}^H \mathbf{p}_m|^2}_{\gamma_{c,k}^{\text{FD},[1]}} + \sigma^2} + \underbrace{\frac{\sum_{m \in \mathcal{K}_1} |\tilde{h}_{m,k,i}|^2 P_m}{\sigma^2}}_{\gamma_{c,k}^{\text{FD},[2]}}, \quad (7)$$

$$\gamma_k^{\text{FD}} = \frac{|\tilde{\mathbf{g}}_{k,i}^H \mathbf{p}_k|^2}{\sum_{m \in \mathcal{K}, m \neq k} |\tilde{\mathbf{g}}_{k,i}^H \mathbf{p}_m|^2 + \sigma^2}. \quad (8)$$

With the SINRs of s_0 and s_k in (4), (5), (7), and (8), the achievable common and private rates are obtained as $R_{c,k}^j = \log_2(1 + \gamma_{c,k}^{\text{FD}})$ and $R_k^j = \log_2(1 + \gamma_k^{\text{FD}})$, $j \in \{\text{FE}, \text{FM}\}$. To guarantee all users decode the common stream, the following condition should satisfy [3]:

$$R_c^j = \min\{R_{c,k}^j | k \in \mathcal{K}\}, \quad (9)$$

R_c^j is shared by all users, we denote C_k as the part of R_c^j that is allocated to user- k , it satisfies $\sum_{k \in \mathcal{K}} C_k \leq R_c^j$. Hence, the total achievable rate of user- k is

$$R_{\text{tot},k}^j = R_k^j + C_k, \forall k \in \mathcal{K}. \quad (10)$$

Note that equations (9) and (10) remain applicable for other transmission modes by setting j to FT/HE/HM/HT. In the following discussion of these transmission modes, the equations will not be repeated.

2) *FT*: In FT mode, there are two time slots: all elements of STAR RIS operate in the reflection mode during the first time slot (λ_r) while all elements of STAR RIS operate in the transmission mode during the second time slot ($1 - \lambda_r$). We denote the SINRs for decoding s_0 and s_k in the reflection and transmission time slots respectively as $\gamma_{c,k}^{\text{FD},i}$ and $\gamma_k^{\text{FD},i}$, where $i \in \{r, t\}$. In the reflection time slot, users in \mathcal{K}_r receives signal from the BS and the STAR RIS while users in \mathcal{K}_t receives signal from the BS only. The corresponding SINRs are given as

$$\begin{aligned} \gamma_{c,k}^{\text{FD},r} &= \gamma_{c,k}^{\text{FD}} |_{\boldsymbol{\Theta}_i = \boldsymbol{\Theta}_r}, \quad \gamma_k^{\text{FD},r} = \gamma_k^{\text{FD}} |_{\boldsymbol{\Theta}_i = \boldsymbol{\Theta}_r}, \quad k \in \mathcal{K}_r, \\ \gamma_{c,k}^{\text{FD},t} &= \gamma_{c,k}^{\text{FD}} |_{\boldsymbol{\Theta}_i = \mathbf{0}}, \quad \gamma_k^{\text{FD},t} = \gamma_k^{\text{FD}} |_{\boldsymbol{\Theta}_i = \mathbf{0}}, \quad k \in \mathcal{K}_t, \end{aligned} \quad (11)$$

where $\gamma_{c,k}^{\text{FD}}$ and γ_k^{FD} are defined in (4) and (5), respectively. In the transmission time slot, users in \mathcal{K}_r receives signal from the BS only while users in \mathcal{K}_t receives signal from both BS and STAR RIS. The corresponding SINRs are given as

$$\begin{aligned} \gamma_{c,k}^{\text{FD},t} &= \gamma_{c,k}^{\text{FD}} |_{\boldsymbol{\Theta}_i = \mathbf{0}}, \quad \gamma_k^{\text{FD},t} = \gamma_k^{\text{FD}} |_{\boldsymbol{\Theta}_i = \mathbf{0}}, \quad k \in \mathcal{K}_r, \\ \gamma_{c,k}^{\text{FD},t} &= \gamma_{c,k}^{\text{FD}} |_{\boldsymbol{\Theta}_i = \boldsymbol{\Theta}_t}, \quad \gamma_k^{\text{FD},t} = \gamma_k^{\text{FD}} |_{\boldsymbol{\Theta}_i = \boldsymbol{\Theta}_t}, \quad k \in \mathcal{K}_t \end{aligned} \quad (12)$$

The achievable common and private rates for user- k are given as

$$\begin{aligned} R_{c,k}^{\text{FT}} &= \lambda_r \log_2(1 + \gamma_{c,k}^{\text{FD},r}) + (1 - \lambda_r) \log_2(1 + \gamma_{c,k}^{\text{FD},t}), \\ R_k^{\text{FT}} &= \lambda_r \log_2(1 + \gamma_k^{\text{FD},r}) + (1 - \lambda_r) \log_2(1 + \gamma_k^{\text{FD},t}). \end{aligned} \quad (13)$$

By substituting $R_{c,k}^{\text{FT}}$ and R_k^{FT} into (9) and (10), we obtain the corresponding achievable rate of each user in the FT mode.

D. Received Signal Model for HD-based Transmission Modes

In HD-based transmission modes, the direct and cooperative transmission phases are orthogonal in each transmission block. Contrast to FD-based modes, there is no self-interference at relaying users, but the transmission rates for the direct and transmission phases are scaled by the pre-log factors λ ($0 < \lambda \leq 1$) and $(1 - \lambda)$, respectively. In the following, we specify the received signals and achievable rates for HE, HM, and HT.

1) *HE/HM*: In the direct transmission phase, the signal received at user- k is

$$y_k^{\text{HD},[1]} = \tilde{\mathbf{g}}_{k,i}^H \mathbf{x}^{[1]} + n_k, \forall k \in \mathcal{K}, j \in \{\text{HE}, \text{HM}\}. \quad (14)$$

The SINRs of decoding s_0 and s_k in the direct transmission phase are given as

$$\gamma_{c,k}^{\text{HD},[1]} = \frac{|\tilde{\mathbf{g}}_{k,i}^H \mathbf{p}_0|^2}{\sum_{m \in \mathcal{K}} |\tilde{\mathbf{g}}_{k,i}^H \mathbf{p}_m|^2 + \sigma^2}, \quad (15)$$

$$\gamma_k^{\text{HD}} = \frac{|\tilde{\mathbf{g}}_{k,i}^H \mathbf{p}_k|^2}{\sum_{m \in \mathcal{K}, m \neq k} |\tilde{\mathbf{g}}_{k,i}^H \mathbf{p}_m|^2 + \sigma^2}. \quad (16)$$

In the cooperative transmission phase, users in \mathcal{K}_1 forward the decoded s_0 to users in \mathcal{K}_2 . The signal received at user- k in \mathcal{K}_2 in the cooperative transmission phase is

$$y_k^{\text{HD},[2]} = \sum_{m \in \mathcal{K}_1} \tilde{h}_{m,k,i} \sqrt{P_m} s_0 + n_k, \forall k \in \mathcal{K}_2. \quad (17)$$

The SINR of decoding s_0 at user- k in \mathcal{K}_2 in the cooperative transmission phase is given as

$$\gamma_{c,k}^{\text{HD},[2]} = \frac{\sum_{m \in \mathcal{K}_1} |\tilde{h}_{m,k,i}|^2 P_m}{\sigma^2}. \quad (18)$$

With the SINR in (15), (16), and (18), we obtain the achievable common and private rates in HF and HM modes ($j \in \{\text{HE}, \text{HM}\}$) as

$$\begin{aligned} R_{c,k}^j &= \lambda \log_2(1 + \gamma_{c,k}^{\text{HD},[1]}), \quad \forall k \in \mathcal{K}_1 \\ R_{c,k}^j &= \lambda \log_2(1 + \gamma_{c,k}^{\text{HD},[1]}) + (1 - \lambda) \log_2(1 + \gamma_{c,k}^{\text{HD},[2]}), \quad \forall k \in \mathcal{K}_2 \end{aligned} \quad (19)$$

and

$$R_k^j = \lambda \log_2(1 + \gamma_k^{\text{HD}}). \quad (20)$$

By substituting (19) and (20) into (9) and (10), we obtain the corresponding achievable rate of each user in the HE and HM modes.

2) *HT*: In the HT mode, there are four time slots: two for direct transmission with STAR RIS reflection or transmission, and two for cooperative transmission with STAR RIS reflection or transmission. We use $\gamma_{c,k}^{\text{HD},[s],i}$ and $\gamma_k^{\text{HD},i}$, $i \in \{r, t\}$, $s \in \{1, 2\}$ to denote the SINRs of decoding s_0 and s_k in the direct or cooperative transmission phase. The superscript i indicates whether it's in the reflection or transmission time slot. Specifically, in the two reflection time slots respectively for cooperative and transmission phases, we have

$$\begin{aligned}\gamma_{c,k}^{\text{HD},[s],r} &= \gamma_{c,k}^{\text{HD},[s]} |_{\Theta_i=\Theta_r}, \quad \gamma_k^{\text{HD},r} = \gamma_k^{\text{HD}} |_{\Theta_i=\Theta_r}, \quad k \in \mathcal{K}_r, \\ \gamma_{c,k}^{\text{HD},[s],r} &= \gamma_{c,k}^{\text{HD},[s]} |_{\Theta_i=0}, \quad \gamma_k^{\text{HD},r} = \gamma_k^{\text{HD}} |_{\Theta_i=0}, \quad k \in \mathcal{K}_t,\end{aligned}\quad (21)$$

where $\gamma_{c,k}^{\text{HD},[s]}$, $s \in \{1, 2\}$ and γ_k^{FD} are defined in (15), (18), and (16), and respectively. In the two transmission time slots respectively for cooperative and transmission phases, we have

$$\begin{aligned}\gamma_{c,k}^{\text{HD},[s],t} &= \gamma_{c,k}^{\text{HD},[s]} |_{\Theta_i=0}, \quad \gamma_k^{\text{HD},t} = \gamma_k^{\text{HD}} |_{\Theta_i=0}, \quad k \in \mathcal{K}_r, \\ \gamma_{c,k}^{\text{HD},[s],t} &= \gamma_{c,k}^{\text{HD},[s]} |_{\Theta_i=\Theta_t}, \quad \gamma_k^{\text{HD},t} = \gamma_k^{\text{HD}} |_{\Theta_i=\Theta_t}, \quad k \in \mathcal{K}_t.\end{aligned}\quad (22)$$

Hence, the achievable common and private rates for user- k are given as

$$R_{c,k}^{\text{HT}} = \lambda_1 \log_2 \left(1 + \gamma_{c,k}^{\text{HD},[1],r} \right) + \lambda_2 \log_2 \left(1 + \gamma_{c,k}^{\text{HD},[1],t} \right), \quad \forall k \in \mathcal{K}_1,$$

$$\begin{aligned}R_{c,k}^{\text{HT}} &= \lambda_1 \log_2 \left(1 + \gamma_{c,k}^{\text{HD},[1],r} \right) \\ &+ (\lambda_r - \lambda_1) \log_2 \left(1 + \gamma_{c,k}^{\text{HD},[2],r} \right) \\ &+ \lambda_2 \log_2 \left(1 + \gamma_{c,k}^{\text{HD},[1],t} \right) \\ &+ (1 - \lambda_r - \lambda_2) \log_2 \left(1 + \gamma_{c,k}^{\text{HD},[2],t} \right), \quad \forall k \in \mathcal{K}_2.\end{aligned}\quad (23)$$

$$R_k^{\text{HT}} = \lambda_1 \log_2 \left(1 + \gamma_k^{\text{HD},r} \right) + \lambda_2 \log_2 \left(1 + \gamma_k^{\text{HD},t} \right). \quad (24)$$

E. Problem Formulation

In this work, we aim to jointly optimize the active beamforming \mathbf{P} at the BS, the common rate allocation $\mathbf{c} = [C_1, \dots, C_K]$, as well as the passive beamforming Θ_r , Θ_t at the STAR RIS. For the HD-based transmission modes, the corresponding time allocation coefficients are also jointly optimized. Our objective is to maximize the minimum user rate (max-min rate) among all users subject to the transmit power constraint. The formulated problems for the six transmission modes of the proposed STAR RIS-aided CRS model are illustrated as follows:

1) *FE*: $j = \text{FE}$, the optimization problem is formulated as

$$\mathcal{P}_{\text{FE}} : \max_{\mathbf{P}, \mathbf{c}, \Theta_r, \Theta_t} \min_{k \in \mathcal{K}} R_{\text{tot},k}^{\text{FE}} \quad (25a)$$

$$\text{s.t.} \quad \sum_{k \in \mathcal{K}} C_k \leq R_c^j, C_k \geq 0, \forall k \in \mathcal{K} \quad (25b)$$

$$\theta_{n,i} \in [0, 2\pi), \forall n \in \mathcal{N}, i \in \{r, t\}, \quad (25c)$$

$$\text{tr}(\mathbf{P}\mathbf{P}^H) \leq P_t \quad (25d)$$

$$\beta_{n,r}, \beta_{n,t} \in [0, 1], \beta_{n,r} + \beta_{n,t} = 1, \forall n \in \mathcal{N}, \quad (25e)$$

where constraint (25b) guarantees the common stream is successfully decoded by all users. Constraints (25c) and (25e) are the constraints for the phase shift and amplitude ranges for each element of the STAR RIS, respectively. (25d) limits the transmit power at the BS.

2) *FM*: $j = \text{FM}$, the formulated problem is given as

$$\mathcal{P}_{\text{FM}} : \max_{\mathbf{P}, \mathbf{c}, \Theta_r, \Theta_t} \min_{k \in \mathcal{K}} R_{\text{tot},k}^{\text{FM}} \quad (26a)$$

$$\text{s.t.} \quad (25b)-(25d)$$

$$\beta_{n,r}, \beta_{n,t} \in \{0, 1\}, \beta_{n,r} + \beta_{n,t} = 1, \forall n \in \mathcal{N}. \quad (26b)$$

3) *FT*: $j = \text{FT}$, the time allocation variable λ_r is jointly optimized with the beamforming matrices and the common rate allocation. The optimization problem is

$$\mathcal{P}_{\text{FT}} : \max_{\mathbf{P}, \mathbf{c}, \Theta_r, \Theta_t, \lambda_r} \min_{k \in \mathcal{K}} R_{\text{tot},k}^{\text{FT}} \quad (27a)$$

$$\text{s.t.} \quad (25b)-(25d),$$

$$\beta_{n,r}, \beta_{n,t} \in [0, 1], \forall n \in \mathcal{N}, \quad (27b)$$

$$0 \leq \lambda_r \leq 1. \quad (27c)$$

4) *HE*: $j = \text{HE}$, the time allocation variable λ is jointly optimized with the beamforming matrices and the common rate allocation. The formulated problem is

$$\mathcal{P}_{\text{HE}} : \max_{\mathbf{P}, \mathbf{c}, \Theta_r, \Theta_t, \lambda} \min_{k \in \mathcal{K}} R_{\text{tot},k}^{\text{HE}} \quad (28a)$$

$$\text{s.t.} \quad (25b)-(25e)$$

$$0 < \lambda \leq 1. \quad (28b)$$

5) *HM*: $j = \text{HM}$, the corresponding optimization problem is formulated as

$$\mathcal{P}_{\text{HM}} : \max_{\mathbf{P}, \mathbf{c}, \Theta_r, \Theta_t, \lambda} \min_{k \in \mathcal{K}} R_{\text{tot},k}^{\text{HM}} \quad (29a)$$

$$\text{s.t.} \quad (25b)-(25d), (26b), (28b).$$

6) *HT*: $j = \text{HT}$, $\lambda_r, \lambda_1, \lambda_2$ are jointly optimized. The corresponding optimization problem is formulated as

$$\mathcal{P}_{\text{HT}} : \max_{\mathbf{P}, \mathbf{c}, \Theta_r, \Theta_t, \lambda_r, \lambda_1, \lambda_2} \min_{k \in \mathcal{K}} R_{\text{tot},k}^{\text{HT}} \quad (30a)$$

$$\text{s.t.} \quad (25b)-(25d), (27b), (27c)$$

$$0 < \lambda_1 \leq \lambda_r, 0 < \lambda_2 \leq 1 - \lambda_r. \quad (30b)$$

From problems (25)-(30) for the six transmission modes, we observe that \mathbf{P} , Θ_r , Θ_t are highly coupled in the non-convex and fractional expressions for the achievable common and private rates. Besides, problem (26) and (29) involve integer programming due to (25b). All problems are highly non-convex and difficult to solve. In the next section, we will propose two algorithm to solve the problems.

III. PROPOSED OPTIMIZATION FRAMEWORKS

To solve the aforementioned six non-convex optimization problems, in this section, we first propose an AO framework that alternatively optimizes the STAR RIS passive beamforming matrices Θ_r and Θ_t , and the remaining variables. To ease the computational complexity, we further propose a low-complexity algorithm to address the optimization problems.

A. Proposed AO Algorithm

We divide the original non-convex problems into two sub-problems, one for the STAR RIS passive beamforming design, the other for the joint BS active beamforming, common rate, and time allocation design. The approaches for solving the two subproblems are detailed in the following:

1) *STAR RIS passive beamforming optimization*: With the transmit beamforming \mathbf{P} , common rate allocation \mathbf{c} and time allocation variables λ_t , λ_1 and λ_2 fixed, we focus on optimizing Θ_r and Θ_t . First, we introduce an auxiliary variable t^j to represent the objective function for the transmission mode j , leading to the following constraint:

$$R_{p,k}^j + C_k \geq t^j, \forall k \in \mathcal{K}, j \in \{\text{FE, FM, FT, HE, HM, HT}\}. \quad (31)$$

Although the achievable rate expressions may vary across different transmission modes, our main focus is the SINR expressions as the optimization variables Θ_r and Θ_t are embedded solely within the SINR. Note that the non-convexity of the SINR expressions remains consistent across all six transmission modes. The key distinction in optimizing the STAR RIS across these modes lies in the constraints imposed by the ES, MS, and TS protocols.

In the following, we begin by illustrating the SCA-based method employed to address the non-convexity of the SINR expressions, using the FE mode as an example. Following this, we elaborate the penalty methods proposed to manage the STAR RIS constraints for the ES, MS, and TS protocols, respectively.

• Step 1.1: The SCA method for non-convex SINRs:

Let $\psi_{n,i} = \sqrt{\beta_{n,i}} e^{j\theta_{n,i}}, n \in \mathcal{N}, i \in \{r, t\}$ denote each element of Θ_r and Θ_t . With $\boldsymbol{\psi}_i = [\psi_{1,i}, \dots, \psi_{N,i}]^T$, we have $\mathbf{g}_k^H \mathbf{p}_m + \mathbf{h}_k^H \Theta_i \mathbf{E} \mathbf{p}_m = \bar{g}_{km} + \mathbf{s}_{km}^H \boldsymbol{\psi}_i$, $\mathbf{h}_n^H \Theta_i \mathbf{h}_m = \bar{h}_{m,n} + \mathbf{s}_{m,n}^H \boldsymbol{\psi}_i$, where $\bar{g}_{km} = \mathbf{g}_k^H \mathbf{p}_m$, $\mathbf{s}_{km} = (\text{diag}(\mathbf{h}_k^H) \mathbf{E} \mathbf{p}_m)^*$ and $\bar{h}_{m,n} = (\text{diag}(\mathbf{h}_n^H) \mathbf{h}_m)^* \in \mathbb{C}^{N \times 1}$. In this way, the optimization variables are represented by $\boldsymbol{\psi}_r$ and $\boldsymbol{\psi}_t$.

Taking the FE problem (25) as an example, we first introduce slack variables $\boldsymbol{\delta} = [\delta_1, \dots, \delta_K]^T$ and $\boldsymbol{\delta}_c = [\delta_{c,1}, \dots, \delta_{c,K}]^T$ to respectively denote the SINRs of s_k and s_0 in the direct transmission phase. Furthermore, we introduce $\boldsymbol{\xi} = [\xi_1, \dots, \xi_{K_2}]$ to denote the SINRs of the destination users in the cooperative transmission phase, where K_2 is the number of users in \mathcal{K}_2 . The optimization problem (25) for updating the STAR RIS passive beamforming matrices is then equivalently transformed into

$$\mathcal{P}_{\text{FE-1}}: \max_{t^{\text{FE}}, \boldsymbol{\psi}_r, \boldsymbol{\psi}_t, \boldsymbol{\delta}, \boldsymbol{\delta}_c, \boldsymbol{\xi}} t^{\text{FE}} \quad (32a)$$

$$\text{s.t. } \log_2(1 + \delta_k) + C_k \geq t^{\text{FE}}, \forall k \in \mathcal{K}, \quad (32b)$$

$$\log_2(1 + \delta_{c,k}) \geq \sum_{m \in \mathcal{K}} C_m, k \in \mathcal{K}_1, \quad (32c)$$

$$\log_2(1 + \delta_{c,k} + \xi_k) \geq \sum_{m \in \mathcal{K}} C_m, k \in \mathcal{K}_2, \quad (32d)$$

$$\delta_{c,k} \leq \gamma_{c,k}^{\text{FD},[1]}, \forall k \in \mathcal{K}, \quad (32e)$$

$$\delta_k \leq \gamma_k^{\text{FD}}, \forall k \in \mathcal{K}, \quad (32f)$$

$$\xi_k \leq \gamma_{c,k}^{\text{FD},[2]}, \forall k \in \mathcal{K}_2, \quad (32g)$$

$$(25e).$$

For constraints (32e) and (32f), we further introduce slack variables $\boldsymbol{\eta} = [\eta_1, \dots, \eta_K]^T$ and $\boldsymbol{\eta}_c = [\eta_{c,1}, \dots, \eta_{c,K}]^T$ to respectively denote the denominators of the SINRs for s_0 and s_k . (32e) and (32f) are equivalently transformed to

$$\eta_{c,k} \geq \text{de}(\gamma_{c,k}^{\text{FD},[1]}), \forall k \in \mathcal{K} \quad (33a)$$

$$\eta_k \geq \text{de}(\gamma_k^{\text{FD}}), \forall k \in \mathcal{K} \quad (33b)$$

$$\delta_{c,k} \eta_{c,k} \leq |\bar{g}_{k0} + \mathbf{s}_{k0}^H \boldsymbol{\psi}_i|^2, \quad (33c)$$

$$\delta_k \eta_k \leq |\bar{g}_{kk} + \mathbf{s}_{kk}^H \boldsymbol{\psi}_i|^2, \quad (33d)$$

where $\text{de}(\cdot)$ is an operator defined to extract the denominator of a fraction, i.e., $\text{de}(\frac{a}{b}) = b$. For constraint (33c), the left-hand side (LHS) equals to $\delta_{c,k} \eta_{c,k} = \frac{1}{4}(\delta_{c,k} + \eta_{c,k})^2 - \frac{1}{4}(\delta_{c,k} - \eta_{c,k})^2$. By further approximating $\delta_{c,k} \eta_{c,k}$ at the point $(\delta_{c,k}^{[z]}, \eta_{c,k}^{[z]})$ in iteration $[z]$ using the first-order Taylor approximation of $(\delta_{c,k} - \eta_{c,k})^2$, we have

$$\begin{aligned} \delta_{c,k} \eta_{c,k} &\leq \frac{1}{4}(\delta_{c,k} + \eta_{c,k})^2 - \frac{1}{2}(\delta_{c,k}^{[z]} - \eta_{c,k}^{[z]})(\delta_{c,k} - \eta_{c,k}) \\ &\quad + \frac{1}{4}(\delta_{c,k}^{[z]} - \eta_{c,k}^{[z]})^2 \triangleq \nu(\delta_{c,k}^{[z]}, \eta_{c,k}^{[z]}). \end{aligned} \quad (34)$$

We also approximate the right-hand side (RHS) of (33c) at $\boldsymbol{\psi}_i^{[z]}$ by the first-order Taylor approximation of $|\bar{g}_{k0} + \mathbf{s}_{k0}^H \boldsymbol{\psi}_i|^2$ as

$$\begin{aligned} |\bar{g}_{k0} + \mathbf{s}_{k0}^H \boldsymbol{\psi}_i|^2 &\geq 2\Re\{(\mathbf{s}_{k0}^H \boldsymbol{\psi}_i^{[z]} + \bar{g}_{k0})^H \mathbf{s}_{k0}^H \boldsymbol{\psi}_i\} - |\mathbf{s}_{k0}^H \boldsymbol{\psi}_i|^2 \\ &\quad + |\bar{g}_{k0}|^2 \triangleq \varpi(\boldsymbol{\psi}_i^{[z]}, \boldsymbol{\psi}_i, \bar{g}_{k0}, \mathbf{s}_{k0}). \end{aligned} \quad (35)$$

Based on this approach, constraints (33c) and (33d) are transformed to

$$\nu(\delta_{c,k}^{[z]}, \eta_{c,k}^{[z]}) \leq \varpi(\boldsymbol{\psi}_i^{[z]}, \boldsymbol{\psi}_i, \bar{g}_{k0}, \mathbf{s}_{k0}), \forall k \in \mathcal{K}_1, \quad (36a)$$

$$\nu(\delta_k^{[z]}, \eta_k^{[z]}) \leq \varpi(\boldsymbol{\psi}_i^{[z]}, \boldsymbol{\psi}_i, \bar{g}_{kk}, \mathbf{s}_{kk}), \forall k \in \mathcal{K}. \quad (36b)$$

And constraint (32g) is approximated as

$$\xi_k \sigma^2 \leq P_m \varpi(\boldsymbol{\psi}_i^{[z]}, \boldsymbol{\psi}_i, h_{m,k}, \mathbf{h}_{m,k}), \forall k \in \mathcal{K} \quad (37)$$

Therefore, utilizing the SCA method, the non-convex SINR expressions (32e)–(32g) are replaced by (36) and (37), which are convex. This approach can be applied directly to other five transmission modes, so we simplify by omitting their discussion here.

• Step 1.2: The penalty method for non-convex STAR RIS constraints:

After Step 1.1, the optimization problems for passive beamforming in all six modes become convex except for the constraints related to the phase and amplitude of the STAR RIS. In the following, we specify the penalty methods proposed to handle these constraints for the ES, MS, and TS protocols.

ES: For constraint (25e), we adopt the penalty method proposed in [27]. By introducing a large positive constant C , the objective function into $t^j + C \sum_{n=1}^N (|\psi_{n,r}|^2 + |\psi_{n,t}|^2 - 1), j \in \{\text{FE, HE}\}$ with an additional constraint

$$|\psi_{n,r}|^2 + |\psi_{n,t}|^2 \leq 1. \quad (38)$$

Algorithm 1: STAR RIS passive beamforming optimization algorithm for six transmission modes

- 1 **Initialize:** $j, z = 0, t^{j,[z]}, \Theta_r^{[z]}, \Theta_t^{[z]}$, and slack variables for mode j ;
 - 2 **repeat**
 - 3 $z \leftarrow z + 1$;
 - 4 Updating $\Theta_r^{[z]}, \Theta_t^{[z]}$ by employing Steps 1.1 and 1.2 to approximate the problem and then solving the approximated convex problem using CVX ;
 - 5 **until** convergence;
-

Using the first-order Taylor approximation of $(|\psi_{n,r}|^2 + |\psi_{n,t}|^2)$ at iteration $[z]$, we obtain the approximated objective function as

$$t^j + C \sum_{n=1}^N \Re\{2(\psi_{n,r}^{[z]})^* \psi_{n,r} - |\psi_{n,r}^{[z]}|^2 + 2(\psi_{n,t}^{[z]})^* \psi_{n,t} - |\psi_{n,t}^{[z]}|^2\}. \quad (39)$$

MS: For constraint (26b), it is obvious that the amplitude coefficient of each STAR RIS element in the FM and HM modes is an integer chosen from 0 and 1. To transform constraints (26b), it's worth noting that no matter each element is 0 or 1, it always satisfies (38) and

$$-|\psi_{n,i}|^2 + |\psi_{n,i}| = 0, i \in \{r, t\}. \quad (40)$$

(40) forces the amplitudes of $\psi_{n,r}$ and $\psi_{n,t}$ to 0 or 1. Due to constraint (38), $0 \leq |\psi_{n,i}| \leq 1$, we obtain that

$$-|\psi_{n,i}|^2 + |\psi_{n,i}| \geq 0, i \in \{r, t\}. \quad (41)$$

Hence, constraint (26b) can be replaced by adding a penalty term to the objective function as $t^j - C \sum_{n=1}^N (-|\psi_{n,r}|^2 + |\psi_{n,r}| - |\psi_{n,t}|^2 + |\psi_{n,t}|)$, $j \in \{FM, HM\}$. Applying the first-order Taylor approximation to the penalty term $-|\psi_{n,r}|^2 - |\psi_{n,t}|^2$ at iteration $[z]$, the objective function is transformed to

$$t^j - C \sum_{n=1}^N \left(A^{[z]} - 2\Re\{(\psi_{n,r}^{[z]})^* \psi_{n,r}\} - 2\Re\{(\psi_{n,t}^{[z]})^* \psi_{n,t}\} \right), \quad (42)$$

where $A^{[z]} = |\psi_{n,r}^{[z]}|^2 + |\psi_{n,t}^{[z]}|^2 + |\psi_{n,r}| + |\psi_{n,t}|$.

TS: For TS modes, we also adopt the penalty method proposed in [27] to address constraints (27b), which transforms the objective function into $t^j + C \sum_{n=1}^N (|\psi_{n,r}|^2 - 1 + |\psi_{n,t}|^2 - 1)$, $j \in \{FT, HT\}$ with an additional constraint

$$|\psi_{n,i}|^2 \leq 1, n \in \mathcal{N}, i \in \{r, t\}. \quad (43)$$

The objective function is then approximated in the same way as (39).

After Steps 1.1 and 1.2, the STAR RIS optimization subproblems for all six transmission modes become convex quadratically constrained quadratic program (QCQP) and can be solved using the CVX optimization toolbox. The detailed process to solve the STAR RIS passive beamforming optimization problem is summarized in Algorithm 1.

2) *Joint optimization of the active beamforming, common rate and time allocation:* Given Θ_r and Θ_t , the effective channels of all users are fixed. To jointly optimize the remaining variables, we first introduce an auxiliary variable x^j to denote the objective function for the transmission mode j , leading to the following constraints:

$$R_{p,k}^j + C_k \geq x^j, \forall k \in \mathcal{K}, j \in \{FE, FM, FT, HE, HM, HT\}. \quad (44)$$

In this subproblem, non-convexity arises from both the fractional SINR expressions and the coupling of time allocation variables within the rate expressions. Both of these challenges are tackled using SCA in the following steps.

• **Step 2.1: The SCA method for time allocation variables:**

In this step, we first specified the SCA methods employed to address the coupled time allocation variables within the rate expressions. Note that in the FE and FM modes, there are no time allocation variables. The non-convexity of the corresponding optimization problems arises solely from the SINR expressions, which are directly addressed in Step 2.2.

FT: To optimize λ_r in problem (27), we first introduce the slack variables $\alpha^i = [\alpha_1^i, \dots, \alpha_K^i]^T$, and $\alpha_c^i = [\alpha_{c,1}^i, \dots, \alpha_{c,K}^i]^T$, $i \in \{r, t\}$ to denote the private and common rates. This allows us to transform (44) and (25b) to

$$\lambda_r \alpha_k^r + (1 - \lambda_r) \alpha_k^t + C_k \geq x^{\text{HT}}, \quad (45a)$$

$$\lambda_r \alpha_{c,k}^r + (1 - \lambda_r) \alpha_{c,k}^t \geq \sum_{m \in \mathcal{K}} C_m, \quad (45b)$$

$$\alpha_k^i \leq \log_2(1 + \gamma_k^{\text{FD},i}), \quad (45c)$$

$$\alpha_{c,k}^i \leq \log_2(1 + \gamma_{c,k}^{\text{FD},i}), \quad (45d)$$

For the bilinear function $\lambda_r \alpha_k^r$, it can be approximated by the first-order Taylor approximation at iteration $[z]$ based on $\nu(\cdot)$ in (34). Hence, constraints (45a) and (45b) are approximated as

$$-\nu(\alpha_k^{r,[z]}, -\lambda_r) + \alpha_k^t - \nu(\alpha_k^{t,[z]}, -\lambda_r) + C_k \geq x^{\text{HT}}, \quad (46a)$$

$$-\nu(\alpha_{c,k}^{r,[z]}, -\lambda_r) + \alpha_{c,k}^t - \nu(\alpha_{c,k}^{t,[z]}, -\lambda_r) \geq \sum_{m \in \mathcal{K}} C_m. \quad (46b)$$

HE/HM: To optimize λ in problems (28) and (29), akin to the FT mode, we introduce the slack variables α , and α_c^i to represent the private and common rates, thereby facilitating the transformation of (44) and (25b) to

$$\lambda \alpha_k + C_k \geq x^j, \quad (47a)$$

$$\lambda \alpha_{c,k} \geq \sum_{m \in \mathcal{K}} C_m, k \in \mathcal{K}_1 \quad (47b)$$

$$\lambda \alpha_{c,k} + (1 - \lambda) \log(1 + \gamma_{c,k}^{\text{HD},[2]}) \geq \sum_{m \in \mathcal{K}} C_m, k \in \mathcal{K}_2 \quad (47c)$$

$$\alpha_k \leq \log_2(1 + \gamma_k^{\text{HD}}), \quad (47d)$$

$$\alpha_{c,k} \leq \log_2(1 + \gamma_{c,k}^{\text{HD},[1]}), \quad (47e)$$

Using the same first-order Taylor approximation method in (46), constraints (47a)–(47c) are approximated to

$$-\nu(\alpha_k^{[z]}, -\lambda) + C_k \geq x^j, \quad (48)$$

$$-\nu(\alpha_{c,k}^{[z]}, -\lambda) \geq \sum_{m \in \mathcal{K}} C_m, \forall k \in \mathcal{K}_1, \quad (49)$$

$$-\nu(\alpha_{c,k}^{[z]}, -\lambda) + (1 - \lambda) \log_2(1 + \gamma_{c,k}^{\text{HD},[2]}) \geq \sum_{m \in \mathcal{K}} C_m, \quad (50)$$

$\forall k \in \mathcal{K}_2.$

HT: To jointly optimize λ_r , λ_1 , and λ_2 in problems (28), we also introduce the slack variables α^i , and α_c^i , $i \in \{r, t\}$ to transform the problem. By applying the approximation method described in (46), we approximate (44) and (25b) to

$$-\nu(\alpha_k^{r,[z]}, -\lambda_1) - \nu(\alpha_k^{t,[z]}, -\lambda_2) + C_k \geq x^{\text{FT}}, \quad (51a)$$

$$-\nu(\alpha_{c,k}^{r,[z]}, -\lambda_1) - \nu(\alpha_{c,k}^{t,[z]}, -\lambda_2) \geq \sum_{m \in \mathcal{K}} C_m, \forall k \in \mathcal{K}_1, \quad (51b)$$

$$-\nu(\alpha_{c,k}^{r,[z]}, -\lambda_1) + (\lambda_r - \lambda_1) \log_2(1 + \gamma_{c,k}^{\text{HD},[2],r}) - \nu(\alpha_{c,k}^{t,[z]}, -\lambda_2) + (1 - \lambda_r - \lambda_2) \log_2(1 + \gamma_{c,k}^{\text{HD},[2],t}) \geq \sum_{m \in \mathcal{K}} C_m, \forall k \in \mathcal{K}_2, \quad (51c)$$

$$\alpha_{c,k}^i \geq \log(1 + \gamma_{c,k}^{\text{HD},[1],i}), \quad (51d)$$

$$\alpha_k^i \geq \log(1 + \gamma_k^{\text{HD},i}). \quad (51e)$$

Following Step 2.1, the time allocation variables are decoupled from the non-convex SINR expressions for all transmission modes. Next, we proceed to address the classical non-convex SINR expressions.

• **Step 2.2: The SCA method for non-convex SINRs:**

Similar to Step 1.1, the SCA method for SINRs is applicable to all transmission modes. Therefore, we illustrate this approach using the FE problem (25) as an example, without detailing other modes.

We first introduce slack variables $\iota = [\iota_1, \dots, \iota_K]^T$, $\iota_c = [\iota_{c,1}, \dots, \iota_{c,K}]^T$ to denote the SINRs of s_k and s_0 . Constraints (44) and (25b) are equivalently transformed to

$$\log_2(1 + \iota_k) + C_k \geq x^{\text{FE}}, \forall k \in \mathcal{K}, \quad (52a)$$

$$\log_2(1 + \iota_{c,k}) \geq \sum_{m \in \mathcal{K}} C_m, k \in \mathcal{K}, \quad (52b)$$

$$\iota_{c,k} \leq \gamma_{c,k}^{\text{FD},[1]}, \forall k \in \mathcal{K}, \quad (52c)$$

$$\iota_k \leq \gamma_k^{\text{FD}}, \forall k \in \mathcal{K}. \quad (52d)$$

Constraints (52c) and (52d) remain non-convex, we then introduce variables $\zeta = [\zeta_1, \dots, \zeta_K]^T$, $\zeta_c = [\zeta_{c,1}, \dots, \zeta_{c,K}]^T$ to respectively denote the denominators of SINRs for s_k and s_0 . (52c) and (52d) are equivalently transformed to

$$\zeta_{c,k} \geq \text{de}(\gamma_{c,k}^{\text{FD},[1]}), \forall k \in \mathcal{K}, \quad (53a)$$

$$\zeta_k \geq \text{de}(\gamma_k^{\text{FD}}), \forall k \in \mathcal{K}, \quad (53b)$$

$$\iota_{c,k} \zeta_{c,k} \leq |\tilde{\mathbf{g}}_{i,k}^H \mathbf{p}_0|^2, \quad (53c)$$

$$\iota_k \zeta_k \leq |\tilde{\mathbf{g}}_{i,k}^H \mathbf{p}_k|^2. \quad (53d)$$

Following the approaches specified in Step 1.1 to address the non-convexity in (33), we approximate constraints (53c) and (53d) at iteration $[z]$ to

$$\nu(\iota_{c,k}^{[z]}, \zeta_{c,k}^{[z]}) \leq \varpi(\mathbf{p}_0^{[z]}, \mathbf{p}_0, 0, \tilde{\mathbf{g}}_{i,k}), \forall k \in \mathcal{K}, \quad (54a)$$

$$\nu(\iota_k^{[z]}, \zeta_k^{[z]}) \leq \varpi(\mathbf{p}_k^{[z]}, \mathbf{p}_k, 0, \tilde{\mathbf{g}}_{i,k}), \forall k \in \mathcal{K}. \quad (54b)$$

Algorithm 2: Joint transmit active beamforming and resource allocation algorithm

```

1 Initialize:  $j, z = 0, x^{j,[z]}, \mathbf{P}^{[z]}, \mathbf{c}^{[z]}, \lambda_r^{[z]}, \lambda^{[z]}, \lambda_1^{[z]}, \lambda_2^{[z]}$ 
   and slack variables according to corresponding mode
    $j$ ;
2 repeat
3    $z \leftarrow z + 1$ ;
4   Updating  $\mathbf{P}^{[z]}, \mathbf{c}^{[z]}, \lambda_r^{[z]}, \lambda^{[z]}, \lambda_1^{[z]}, \lambda_2^{[z]}$  uses the
   SCA methods in Steps 2.1 and 2.2;
5 until convergence;
```

Algorithm 3: Proposed AO algorithm

```

1 Initialize:  $j, z = 0, \Theta_r^{[z]}, \Theta_t^{[z]}, \mathbf{P}^{[z]}, \mathbf{c}^{[z]}, \lambda_r^{[z]}, \lambda^{[z]},$ 
    $\lambda_1^{[z]}, \lambda_2^{[z]}$ ;
2 repeat
3    $z \leftarrow z + 1$ 
4   Given  $\mathbf{P}^{[z-1]}, \mathbf{c}^{[z]}, \lambda_r^{[z]}, \lambda^{[z]}, \lambda_1^{[z]}, \lambda_2^{[z]}$ , use
   Algorithm 1 to obtain  $\Theta_t^{[z]}$  and  $\Theta_r^{[z]}$ .
5   Given  $\Theta_t^{[z]}$  and  $\Theta_r^{[z]}$ , use Algorithm 2 to obtain
    $\mathbf{P}^{[z]}, \mathbf{c}^{[z]}, \lambda_r^{[z]}, \lambda^{[z]}, \lambda_1^{[z]}, \lambda_2^{[z]}$ .
6 until convergence;
```

Based on the approximation methods specified in Step 2.1 and 2.2, the joint active beamforming, common rate, and time allocation optimization problems for all six transmission modes become QCQP and can be solved using CVX. The detailed process of the SCA methods to solve this subproblem is illustrated in Algorithm 2.

3) *Alternative Optimization:* Based on Algorithm 1 and Algorithm 2, the proposed AO algorithm that solves the two subproblems iteratively is shown in Algorithm 3. Starting from a feasible point $(\mathbf{P}^{[0]}, \Theta_r^{[0]}, \Theta_t^{[0]}, \mathbf{c}^{[0]}, \lambda_r^{[0]}, \lambda^{[0]}, \lambda_1^{[0]}, \lambda_2^{[0]})$, at each iteration $[z]$, we first update $\Theta_r^{[z]}$ and $\Theta_t^{[z]}$ by Algorithm 1. Given $\Theta_r^{[z]}$ and $\Theta_t^{[z]}$, we then update $\mathbf{P}^{[z]}$, common rate and time allocation based on Algorithm 2. By iteratively solving these two subproblems, the objective function is updated until convergence.

B. Proposed Low-complexity Algorithm

In this subsection, we propose a low-complexity algorithm for the STAR RIS passive beamforming and transmit beamforming optimization subproblems.

1) *STAR RIS passive beamforming optimization:* We begin by specifying the proposed low-complexity algorithm tailored for the ES protocol. Subsequently, we extend this algorithm to the MS and TS protocols.

ES: To develop a low-complexity algorithm for designing Θ_r and Θ_t in the ES protocol, we consider the following problem aimed at maximizing the sum of channel gains:

$$\max_{\Theta_r, \Theta_t} \sum_{k=1}^K \|\mathbf{g}_k^H + \mathbf{h}_k^H \Theta_i \mathbf{E}\|^2, i \in \{r, t\} \quad (55)$$

s.t. (25c), (25e).

Constraints (25c) and (25e) are non-convex, which make the problem (55) difficult to solve. To tackle such a non-convex problem, we first relax constraints (25c) and (25e) to $\|\Theta_r\|_F^2 + \|\Theta_t\|_F^2 \leq N$, where $\|\cdot\|_F$ denotes the Frobenius norm. This approximation relaxes the feasible solutions of Θ_r and Θ_t to a convex set $\mathcal{S} = \{(\Theta_r, \Theta_t) \mid \|\Theta_r\|_F^2 + \|\Theta_t\|_F^2 \leq N\}$. Therefore, problem (55) is relaxed to

$$\max_{\Theta} f(\Theta) \triangleq \|\mathbf{G}^H + \mathbf{H}^H \Theta \mathbf{E}_x\|_F^2 \quad (56a)$$

$$\text{s.t. } \Theta \in \mathcal{S}, \quad (56b)$$

where $\Theta = \begin{bmatrix} \Theta_r & \mathbf{0} \\ \mathbf{0} & \Theta_t \end{bmatrix}$, $\mathbf{G} = [\mathbf{G}_r; \mathbf{G}_t]$, $\mathbf{G}_r = \{\mathbf{g}_k \mid k \in \mathcal{K}_r\}$, $\mathbf{G}_t = \{\mathbf{g}_k \mid k \in \mathcal{K}_t\}$, $\mathbf{H} = [\mathbf{H}_r; \mathbf{H}_t]$, $\mathbf{H}_r = \{\mathbf{h}_k \mid k \in \mathcal{K}_r\}$, $\mathbf{H}_t = \{\mathbf{h}_k \mid k \in \mathcal{K}_t\}$ and $\mathbf{E}_x = [\mathbf{E}; \mathbf{E}]$.

Inspired by the method proposed in [28], we employ the gradient decent method at the point $\Theta_0 = \mathbf{0}$ to derive a closed-form solution of (56). The corresponding gradient of $f(\Theta)$ at $\Theta_0 = \mathbf{0}$ is

$$\nabla_{\Theta} f(\Theta_0) = \mathbf{H} \mathbf{G}^H \mathbf{E}_x^H, \quad (57)$$

By using (57) as the decent direction, i.e., $\mathbf{D}_0 = \nabla_{\Theta} f(\Theta_0)$, we then take the Armijo rule to determine the step size α as

$$f(\Theta_0 + \alpha \mathbf{D}_0) \geq f(\Theta_0) + \phi \cdot \alpha \cdot \text{tr}(\nabla_{\Theta} f(\Theta_0)^H \mathbf{D}_0), \quad (58)$$

where $\phi \in (0, 0.5)$ is a constant shrinkage factor. Substituting (57) into (58), we obtain

$$\alpha^2 \|\mathbf{H}^H \mathbf{H} \mathbf{G}^H \mathbf{E}_x^H \mathbf{E}_x\|_F^2 + \alpha \cdot (2 - \phi) \|\mathbf{H} \mathbf{G}^H \mathbf{E}_x^H\|_F^2 \geq 0 \quad (59)$$

To guarantee the solution is on the boundary of the convex set \mathcal{S} , we set $\alpha = \frac{\sqrt{N}}{\|\mathbf{H} \mathbf{G}^H \mathbf{E}_x^H\|_F}$. Then, we obtain the following solution of problem (56) as

$$\Theta = \frac{\sqrt{N}}{\|\mathbf{H} \mathbf{G}^H \mathbf{E}_x^H\|_F} \mathbf{H} \mathbf{G}^H \mathbf{E}_x^H. \quad (60)$$

However, the solution (60) for the relaxed problem (56) may not satisfy the original constraints (25c), (25e). Therefore, we propose to project Θ into the feasible region. Following [28], we first define the operator $\text{sym}(\cdot)$ that projects any square matrix \mathbf{X} to a symmetric matrix, i.e.,

$$\text{sym}(\mathbf{X}) = \frac{1}{2} (\mathbf{X}^T + \mathbf{X}), \quad (61)$$

and the operator $\text{uni}(\cdot)$ which projects an arbitrary matrix \mathbf{X} to a unitary matrix as

$$\text{uni}(\mathbf{X}) = \mathbf{U} \mathbf{V}^H, \quad (62)$$

where \mathbf{U} and \mathbf{V} unitary matrices obtained by the singular value decomposition (SVD) of \mathbf{X} , i.e., $\mathbf{X} = \mathbf{U} \mathbf{S} \mathbf{V}^H$. Consider \mathbf{X} with dimension N and rank R . Then, the unitary matrices \mathbf{U} and \mathbf{V} can be partitioned as $\mathbf{U} = [\mathbf{U}_R, \mathbf{U}_{N-R}]$ and $\mathbf{V} = [\mathbf{V}_R, \mathbf{V}_{N-R}]$, respectively. Based on the operators in (61) and (62), we could then define the symmetric unitary projection as [28]

$$\text{symuni}(\mathbf{X}) = \text{uni}(\text{sym}(\mathbf{X})) = \hat{\mathbf{U}} \mathbf{V}^H, \quad (63)$$

where $\hat{\mathbf{U}} = [\mathbf{U}_R, \mathbf{V}_{N-R}^*]$.

Utilizing the symmetric unitary projection, we then derive a feasible STAR RIS passive beamforming solution Θ . It's

noteworthy that both Θ_r and Θ_t are diagonal matrices, implying that Θ is also diagonal. The diagonal entries of Θ are determined by

$$\text{diag}\{\Theta\} = \text{diag}\left\{\frac{\sqrt{2}}{2} \text{symuni}(\mathbf{H} \mathbf{G}^H \mathbf{E}_x^H)\right\}. \quad (64)$$

Since $\text{symuni}(\mathbf{H} \mathbf{G}^H \mathbf{E}_x^H) \in \mathbb{C}^{2N \times 2N}$ is a unitary matrix, we have $\|\text{symuni}(\mathbf{H} \mathbf{G}^H \mathbf{E}_x^H)\|_F^2 = 2N$. To ensure constraint (25e), we scale each entry with $\frac{\sqrt{2}}{2}$.

MS: For the MS mode, we first utilize (64) to derive Θ_r and Θ_t . As each element can only operate in either reflection or transmission mode, we then compare the reflection and transmission amplitude coefficients of each STAR RIS element. The element with the higher coefficient is designated as 1, while the one with the lower coefficient is designated as 0. Based on (64), the reflection and transmission coefficients of each STAR RIS element is designed as

$$\beta_{r,n} = \begin{cases} 1, & \text{if } |\Theta_{n,n}| - |\Theta_{N+n,N+n}| \geq 0, \\ 0, & \text{if } |\Theta_{n,n}| - |\Theta_{N+n,N+n}| < 0, \end{cases} \forall n \in \mathcal{N} \quad (65)$$

$$\beta_{t,n} = 1 - \beta_{r,n}.$$

TS: For the TS mode, in the reflection time slots, $\Theta_t = \mathbf{0}$, the amplitudes of all elements in Θ_r are 1. The solution of reflection matrix is given as

$$\Theta_r = \text{diag}\{\text{symuni}(\mathbf{H}_r \mathbf{G}_r^H \mathbf{E}_x^H)\}. \quad (66)$$

In the transmission time slots, $\Theta_r = \mathbf{0}$, the transmission matrix is given as

$$\Theta_t = \text{diag}\{\text{symuni}(\mathbf{H}_t \mathbf{G}_t^H \mathbf{E}_x^H)\}. \quad (67)$$

2) *Joint optimization of the active beamforming, common rate and time allocation:* With fixed Θ_r and Θ_t , we aim to simplify the design of the remaining variables. To achieve this, we reduce the optimization dimension by fixing the direction of the precoders. Subsequently, we focus on jointly optimizing the power, common rate, and time allocation variables.

Let $\bar{\mathbf{g}}_k = \mathbf{g}_k / \|\mathbf{g}_k\|$, $\bar{\mathbf{G}} = [\bar{\mathbf{g}}_1, \dots, \bar{\mathbf{g}}_K]$, $\bar{\mathbf{p}}_k = \mathbf{p}_k / \|\mathbf{p}_k\|$, and $\bar{\mathbf{P}} = [\bar{\mathbf{p}}_1, \dots, \bar{\mathbf{p}}_K]$. We transform the active beamformings in the form of $\mathbf{p}_c = \sqrt{\rho_c} \bar{\mathbf{P}}_t \bar{\mathbf{p}}_c$, $\mathbf{p}_k = \sqrt{\rho_k} \bar{\mathbf{P}}_t \bar{\mathbf{p}}_k$, where ρ_c and ρ_k are the power allocation coefficients. For the beamforming direction $\bar{\mathbf{p}}_k$ of the private streams, we adopt zero-forcing (ZF) beamforming, i.e., $\bar{\mathbf{P}} = \bar{\mathbf{G}} (\bar{\mathbf{G}}^H \bar{\mathbf{G}})^{-1}$ [29]. For the beamforming direction $\bar{\mathbf{p}}_c$ of the common stream, we utilize maximum ratio transmission (MRT) and SVD methods as $\bar{\mathbf{p}}_c = \mathbf{u}_c$, where $\mathbf{u}_c = \mathbf{U}_c(:, 1)$, $\mathbf{G} = \mathbf{U}_c \mathbf{S}_c \mathbf{V}_c$ [22]. Based on the aforementioned beamforming direction design, the optimization problems for all six transmission modes are simplified. In the following, we illustrate this simplification by considering the FD mode as a representative example:

$$\max_{\rho, \mathbf{c}} \min_{k \in \mathcal{K}} C_k + R_{p,k}^{\text{FE}} \quad (68a)$$

$$\text{s.t. } \sum_{m \in \mathcal{K}} C_m \leq R_{c,k}^{\text{FE}}, \forall k \in \mathcal{K}, \quad (68b)$$

$$\rho_c + \sum_{k \in \mathcal{K}} \rho_k \leq 1, \quad (68c)$$

where $\rho = [\rho_c, \rho_1, \dots, \rho_K]$ are the power allocation coefficients, $R_{p,k}^{\text{FE}} = \log_2(1 + \rho_k P_t |\bar{\mathbf{g}}_k^H \bar{\mathbf{p}}_k|^2 / \sigma^2)$, $R_{c,k}^{\text{FE}} =$

Algorithm 4: Proposed low-complexity algorithm

- 1 **Initialize:** $j, \mathbf{P}^{[0]}, \mathbf{c}^{[0]}, \lambda_r^{[0]}, \lambda^{[0]}, \lambda_1^{[0]}, \lambda_2^{[0]}$;
 - 2 Update Θ_t and Θ_r through (64) if $j = \text{FE/HE}$, (65) if $j = \text{FM/HM}$, (66) and (67) if $j = \text{FT/HT}$.
 - 3 Given Θ_t and Θ_r , update $\mathbf{P}, \mathbf{c}, \lambda_r, \lambda, \lambda_1, \lambda_2$ by solving the joint power, common rate, and time allocation problem via Algorithm 2.
-

$\log_2(1 + \rho_c P_t |\tilde{\mathbf{g}}_k^H \bar{\mathbf{p}}_c|^2 / (\rho_k P_t |\tilde{\mathbf{g}}_k^H \bar{\mathbf{p}}_k|^2 + \sigma^2))$. The optimization problem can be directly solved using the SCA-based approach specified in Algorithm 2. The optimization approach for other transmission modes aligns with that of the FE mode. For FT/HE/HM/HT modes, the additional time allocation variables are jointly optimized using the SCA-based approach specified in Step 2.1.

The detailed process of the proposed low-complexity algorithm to solve problems (25)–(30) is outlined in Algorithm 4. Contrasted with Algorithm 3, the primary difference lies in the closed-form STAR RIS passive beamforming design and the closed-form active beamforming direction design. Additionally, there is no alternating optimization between the two subproblems. Each subproblem is solved once before the output.

C. Convergence and Computational Complexity Analysis

1) *Convergence Analysis:* In Algorithm 1, the SCA method guarantees that the objective t^j monotonically increases, meaning that $t^{j,[z-1]} \leq t^{j,[z]}$. This arises from the fact that the solution of Θ_r and Θ_t at iteration $[z-1]$ is a feasible point of the STAR RIS problem at iteration $[z]$. Due to STAR RIS power constraint (25e), there is an upper bound for $t^{j,[z]}$. Hence, the convergence of Algorithm 1 is guaranteed. Similarly, in Algorithm 2, the SCA method guarantees that $x^{j,[z-1]} \leq x^{j,[z]}$ since the solution at iteration $[z-1]$ is also a feasible point of the joint optimization problem at iteration $[z]$. Due to the power constraint (25d) at the BS, there is an upper bound for the objective value. Hence, the convergence of the Algorithm 2 is guaranteed. The convergence of Algorithm 1 and Algorithm 2 implies that the objective of the AO algorithm increases monotonically, which guarantees the convergence of Algorithm 3.

2) *Computational complexity of Algorithm 3:* The computational complexity of Algorithm 1 is $\mathcal{O}(N^{3.5} \log_2(1/\epsilon_1))$, where ϵ_1 is the convergence tolerance. The computational complexity of Algorithm 2 is $\mathcal{O}((KN_t)^{3.5} \log_2(1/\epsilon_2))$, where ϵ_2 is the corresponding convergence tolerance. Therefore, the computational complexity of Algorithm 3 is $\mathcal{O}(T(N^{3.5} \log_2(1/\epsilon_1) + (KN_t)^{3.5} \log_2(1/\epsilon_2)))$, where T denotes the number of iterations of the AO algorithm.

3) *Computational complexity of Algorithm 4:* For the proposed low-complexity algorithm, the computational complexity of the STAR RIS passive beamforming design is mainly occupied by the unitary projection with SVD method, which is $\mathcal{O}(N^3)$. For the active beamforming optimization subproblem, the computational complexity is $\mathcal{O}(K^{3.5} \log_2(1/\epsilon_2))$. Therefore, the overall computational complexity of Algorithm

4 is $\mathcal{O}(N^3 + K^{3.5} \log_2(1/\epsilon_2))$, which is significantly lower than that of Algorithm 3.

IV. NUMERICAL RESULTS

In this section, we evaluate the performance of our proposed STAR RIS-assisted CRS system framework along with the two proposed algorithms.

A. Simulation Setting

The setting of simulation follows [30]. Consider a three-dimensional (3D) space, the BS is located at $(0, 0, 0)\text{m}$, the STAR RIS locates at $(0, 50, 0)\text{m}$. Users are randomly distributed within a circle, with the center being the location of the STAR RIS and a radius of $r = 5$ meters. We follow the method in [7] to separate the users into group \mathcal{K}_1 and \mathcal{K}_2 . We only choose one user with the largest channel gain as the relaying user, other users are destination users. The channels between BS and users, as well as between user- m and user- n are assumed to be Rayleigh fading, and are denoted as $\mathbf{g}_k = L_{\text{BU},k} \bar{\mathbf{g}}_k, h_{m,n} = L_{\text{UU}} \bar{h}_{m,n}$, where $L_{\text{BU},k}$ and L_{UU} denote the path loss between the BS and users as well as the path loss between users. $\bar{\mathbf{g}}_k$ and $\bar{h}_{m,n}$ follow the complex Gaussian distribution with a certain variance, i.e., $\bar{\mathbf{g}}_k \sim \mathcal{CN}(0, \sigma_k^2), \bar{h}_{m,n} \sim \mathcal{CN}(0, \sigma_{m,n}^2)$. The channels between the BS and STAR RIS, as well as between STAR RIS and users are assumed to follow the Rician fading model with the Rician factor being 3dB. The path loss for all the aforementioned channels is defined as $L_x = L_0(d_x/d_0)^{-\alpha_x}, x \in \{\text{BU}, \text{UU}, \text{BR}, \text{RU}\}$, where $d_0 = 1\text{m}$ is the reference distance, $L_0 = -30\text{ dB}$ is the path loss at reference distance, d_x is the distance of different channels, and α_x denotes different channel path exponents. The channel path loss exponents between the BS and STAR RIS, as well as between STAR RIS and users are 2.2 [17]. The channel path loss exponent between the BS and users is 3.76 [27]. Besides, the relaying power is $P_k = 0.5P_t$, the convergence tolerance is $\epsilon = 10^{-3}$, and the noise power is $\sigma = -90\text{ dBm}$. All results are obtained by averaging over 100 random channel realizations. The variances of user channels are set to $\sigma_k^2 = 1$ for the relaying user, $\sigma_k^2 = 0.3$ for the destination users, and $\sigma_{m,n}^2 = 1$.

The following schemes are compared in this section:

- **CRS-FE/FM/FT/HE/HM/HT:** This refers to the STAR RIS-assisted CRS for six different transmission modes, as we proposed in Section II.
- **CRS-HD/FD:** This refers to the existing CRS transmission schemes based on the HD or FD protocols without the assistance of STAR RIS [7], [9].
- **RSMA-ES:** This refers to the existing STAR RIS assisted RSMA transmission scheme without user relaying [19]. Here we only consider the ES protocol since it is more general than MS and TS protocols.
- **SDMA-ES:** This refers to the existing STAR RIS assisted SDMA transmission scheme. Again, we only consider the ES protocol.
- **NOMA-ES:** This refers to the existing STAR RIS assisted NOMA transmission scheme [30] with the ES protocol.

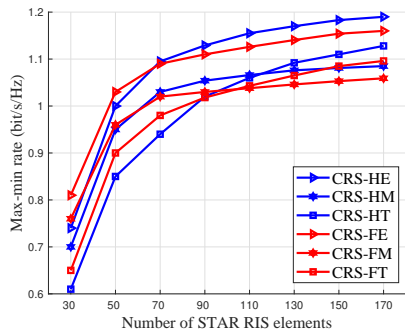


Fig. 3. Max-min rate versus the number of STAR RIS elements N , SNR = 20 dB, $K = 4$, $N_t = 4$.

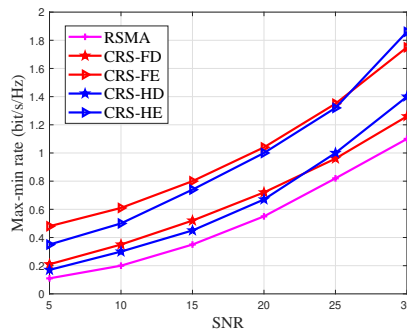


Fig. 4. Max-min rate versus SNR, $N = 50$, $K = 4$, $N_t = 4$.

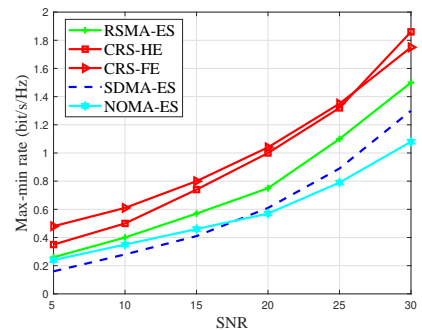


Fig. 5. Max-min rate versus SNR, $N = 50$, $K = 4$, $N_t = 4$.

- **RSMA**: This refers to the conventional 1-layer RSMA transmission scheme, which does not involve user relaying or assistance from STAR RIS [22].

B. Simulation Results

1) Comparison among STAR RIS operating protocols:

From Fig. 3, we observe that the FE/HE mode consistently achieves a higher max-min rate than the FM/HM and FT/HT mode. This is because the ES protocol is more general than the MS and TS protocol, and it ensures that each STAR RIS element has a larger tunable range of the amplitude coefficient. As the number of STAR RIS elements increases, the max-min rate performance gain between FM/HM and FT/HT modes decreases. Surprisingly, when N is larger than 110, the FT/HT mode achieves a higher max-min rate than the FM/HM mode. This indicates that the TS protocol outperforms the MS protocol when the STAR RIS element is large. With an increasing number of STAR RIS elements, the performance improvement gained from having all elements operating within the same transmission/reflection space is outweighed by the performance degradation caused by partial time service.

Due to the superior max-min rate performance of ES compared to MS and TS, in the following simulation results, we only illustrate the proposed STAR RIS-assisted CRS in FE and HE modes for clarity.

2) Comparison between FD and HD relaying protocols:

Fig. 4 illustrates the max-min rate performance versus transmit SNR. We compare our proposed CRS-FE/HE with the conventional RSMA scheme and the conventional CRS schemes with HD and FD protocols. Algorithm 3 is employed to optimize the corresponding problems of the proposed schemes. We set $N = 50$, $K = 4$, $N_t = 4$. The max-min rate increases with SNR for all transmission schemes. It is noteworthy that when SNR is below 25 dB, the CRS-FE scheme achieves a higher max-min rate than the CRS-HE scheme. Conversely, when the SNR exceeds 25 dB, the CRS-HE scheme outperforms the CRS-FE scheme. This divergence stems from the introduction of self-interference in FD relaying. As the SNR increases, the level of self-interference also rises. This indicates that the HD protocol is preferred in the high SNR regime while the FD protocol is preferred in the low and moderate SNR regimes. For consistently ensuring the optimal max-min rate

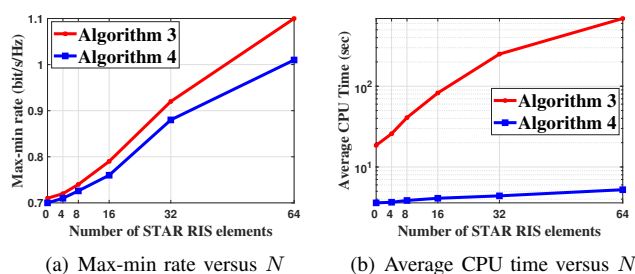


Fig. 6. The performance of the two proposed algorithms.

performance gain, we can employ FD relaying at low and moderate SNR and HD relaying at high SNR.

From Fig. 4, it is obvious that with the assistance of STAR RIS and CRS, CRS-FE/HE achieves explicit max-min rate gain over conventional schemes. Specifically, CRS-FE demonstrates an average relative performance gain of 117.1% and 52.4% over conventional RSMA and CRS-FD, respectively. This demonstrates the significant performance enhancement achieved by integrating STAR RIS and CRS.

3) *Comparison among different MA schemes*: In Fig. 5, we compare various STAR RIS-assisted transmission schemes with the ES protocol when $N = 50$, $K = 4$, $N_t = 4$. The results show that our proposed STAR RIS-aided CRS scheme outperforms other MA schemes. It achieves an average max-min rate gain of 42.6% over the RSMA-ES scheme, 90.9% over the SDMA-ES scheme, and 77.2% over the NOMA-ES scheme. Besides, the RSMA-ES scheme outperforms NOMA-ES and SDMA-ES. By splitting the user message into common and private parts, RSMA facilitates more flexible interference management in all SNR regimes.

4) *Comparison between the two proposed algorithms*: In Fig. 6, we compare the two proposed optimization algorithms for the proposed STAR RIS-aided CRS in the ES mode. We set SNR = 20 dB, $K = 4$, $N_t = 4$. In comparison to the proposed AO algorithm, the low-complexity algorithm reduces the average CPU time by 99.2% while incurring only a 9.1% performance loss at $N = 64$. This confirms the effectiveness of the proposed low-complexity algorithm. This efficiency is primarily due to the low-complexity algorithm eliminating the need for CVX operations to update Θ_r and Θ_t , along with the alternative optimization between two subproblems.

Instead, CVX is exclusively used for joint power, common rate, and time allocation, leading to a significant reduction in optimization dimension. The results suggest that if the system can accommodate high time complexity, Algorithm 3 should be employed to achieve near-optimal max-min rate performance. Conversely, if the system is time sensitive, the low-complexity Algorithm is recommended.

V. CONCLUSION

In this paper, we propose a novel STAR RIS-assisted CRS transmission with six different transmission modes, namely, HE, HM, HT, FE, FM, FT. With the objective of maximizing the minimum user rate, we then propose a unified SCA-based AO algorithm to optimize the BS active beamforming and the STAR RIS passive beamforming iteratively under the transmit power constraint at the BS and the law of energy conservation at the STAR RIS. Meanwhile, we propose a novel low-complexity resource allocation algorithm that designs the BS active beamforming and the STAR RIS passive beamforming in closed form. Numerical results show that our proposed STAR RIS aid-CRS system achieves superior max-min rate performance gain over the existing CRS schemes and the STAR RIS-aided MA schemes. Furthermore, we show that the FD relaying has better max-min rate performance at low and moderate SNR while the HD relaying is preferred at high SNR. The ES protocol offers superior max-min rate performance compared to the MS and TS protocols, albeit with increased hardware complexity. With a large number of STAR RIS elements, the TS protocol demonstrates a significantly higher max-min rate gain compared to the MS protocol. Our proposed AO algorithm is better suited for systems that can accommodate higher time complexity, while the low-complexity algorithm is preferable for systems that are more time sensitive.

REFERENCES

- [1] K. Zhao, Y. Mao, and Y. Shi, "STAR-RIS empowered full duplex cooperative rate splitting," in *IEEE VTC2023-Fall*, 2023, pp. 1–5.
- [2] B. Clerckx, Y. Mao, E. A. Jorswieck, J. Yuan, D. J. Love, E. Erkip, and D. Niyato, "A primer on rate-splitting multiple access: Tutorial, myths, and frequently asked questions," *IEEE J. Sel. Areas Commun.*, May 2023.
- [3] Y. Mao, B. Clerckx, and V. O. K. Li, "Rate-splitting multiple access for downlink communication systems: Bridging, generalizing, and outperforming SDMA and NOMA," *EURASIP J. Wireless Commun. Netw.*, vol. 2018, no. 1, p. 133, May 2018.
- [4] Y. Mao, B. Clerckx, and V. O. Li, "Rate-splitting for multi-antenna non-orthogonal unicast and multicast transmission: Spectral and energy efficiency analysis," *IEEE Trans. Commun.*, vol. 67, no. 12, pp. 8754–8770, Sep 2019.
- [5] B. Clerckx, Y. Mao, R. Schober, and H. V. Poor, "Rate-splitting unifying SDMA, OMA, NOMA, and multicasting in MISO broadcast channel: A simple two-user rate analysis," *IEEE Wireless Commun. Lett.*, vol. 9, no. 3, pp. 349–353, Nov. 2019.
- [6] J. Zhang, B. Clerckx, J. Ge, and Y. Mao, "Cooperative rate splitting for MISO broadcast channel with user relaying, and performance benefits over cooperative NOMA," *IEEE Signal Process. Lett.*, vol. 26, no. 11, pp. 1678–1682, Nov. 2019.
- [7] Y. Mao, B. Clerckx, J. Zhang, V. O. K. Li, and M. A. Arafath, "Max-min fairness of k -user cooperative rate-splitting in MISO broadcast channel with user relaying," *IEEE Trans. Wireless Commun.*, vol. 19, no. 10, pp. 6362–6376, Oct. 2020.
- [8] S. Khisa, M. Almekhlafi, M. Elhattab, and C. Assi, "Full duplex cooperative rate splitting multiple access for a MISO broadcast channel with two users," *IEEE Commun. Lett.*, vol. 26, no. 8, pp. 1913–1917, May 2022.
- [9] T. Li, H. Zhang, X. Zhou, and D. Yuan, "Full-duplex cooperative rate-splitting for multigroup multicast with SWIPT," *IEEE Trans. Wireless Commun.*, vol. 21, no. 6, pp. 4379–4393, Nov 2021.
- [10] Q. Pan, J. Wu, X. Zheng, W. Yang, and J. Li, "Differential privacy and IRS empowered intelligent energy harvesting for 6G internet of things," *IEEE Internet Things J.*, vol. 9, no. 22, pp. 22 109–22 122, Aug 2021.
- [11] E. Basar, M. Di Renzo, J. De Rosny, M. Debbah, M.-S. Alouini, and R. Zhang, "Wireless communications through reconfigurable intelligent surfaces," *IEEE Access*, vol. 7, pp. 116 753–116 773, Aug 2019.
- [12] Z. Li, W. Yuan, B. Li, J. Wu, C. You, and F. Meng, "Reconfigurable intelligent surface aided OTFS: Transmission scheme and channel estimation," *IEEE Internet Things J.*, Apr 2023.
- [13] Y. Liu, X. Mu, J. Xu, R. Schober, Y. Hao, H. V. Poor, and L. Hanzo, "STAR: Simultaneous transmission and reflection for 360° coverage by intelligent surfaces," *IEEE Wireless Commun.*, vol. 28, no. 6, pp. 102–109, Dec 2021.
- [14] H. Zhang and B. Di, "Intelligent omni-surfaces: Simultaneous refraction and reflection for full-dimensional wireless communications," *IEEE Commun. Surv. Tut.*, Aug 2022.
- [15] C. Wu, Y. Liu, X. Mu, X. Gu, and O. A. Dobre, "Coverage characterization of STAR-RIS networks: NOMA and OMA," *IEEE Commun. Lett.*, vol. 25, no. 9, pp. 3036–3040, Jun. 2021.
- [16] Z. Zhang, J. Chen, Y. Liu, Q. Wu, B. He, and L. Yang, "On the secrecy design of STAR-RIS assisted uplink NOMA networks," *IEEE Trans. Wireless Commun.*, vol. 21, no. 12, pp. 11 207–11 221, Jul. 2022.
- [17] J. Zuo, Y. Liu, Z. Ding, L. Song, and H. V. Poor, "Joint design for simultaneously transmitting and reflecting (STAR) RIS assisted NOMA systems," *IEEE Trans. Wireless Commun.*, vol. 22, no. 1, pp. 611–626, Aug. 2022.
- [18] H. R. Hashempour, H. Bastami, M. Moradikia, S. A. Zekavat, H. Behroozi, and A. L. Swindlehurst, "Secure SWIPT in STAR-RIS aided downlink MISO rate-splitting multiple access networks," *arXiv preprint arXiv:2211.09081*, Nov 2022.
- [19] M. Katwe, K. Singh, B. Clerckx, and C.-P. Li, "Improved spectral efficiency in STAR-RIS aided uplink communication using rate splitting multiple access," *IEEE Trans. Wireless Commun.*, Jan. 2023.
- [20] S. Dhok and P. K. Sharma, "Rate-splitting multiple access with STAR RIS over spatially-correlated channels," *IEEE Trans. Commun.*, vol. 70, no. 10, pp. 6410–6424, Aug. 2022.
- [21] B. Clerckx, H. Joudeh, C. Hao, M. Dai, and B. Rassouli, "Rate splitting for MIMO wireless networks: A promising PHY-layer strategy for LTE evolution," *IEEE Commun. Mag.*, vol. 54, no. 5, pp. 98–105, May 2016.
- [22] Y. Mao, O. Dizdar, B. Clerckx, R. Schober, P. Popovski, and H. V. Poor, "Rate-splitting multiple access: Fundamentals, survey, and future research trends," *IEEE Commun. Surv. Tut.*, Jun. 2022.
- [23] T. Riihonen, S. Werner, and R. Wichman, "Mitigation of loopback self-interference in full-duplex MIMO relays," *IEEE Trans. Signal Process.*, vol. 59, no. 12, pp. 5983–5993, Dec. 2011.
- [24] A. Sabharwal, P. Schniter, D. Guo, D. W. Bliss, S. Rangarajan, and R. Wichman, "In-band full-duplex wireless: Challenges and opportunities," *IEEE J. Sel. Areas Commun.*, vol. 32, no. 9, pp. 1637–1652, Sep. 2014.
- [25] C. Zhong, H. A. Suraweera, G. Zheng, I. Krikidis, and Z. Zhang, "Wireless information and power transfer with full duplex relaying," *IEEE Trans. Commun.*, vol. 62, no. 10, pp. 3447–3461, Oct. 2014.
- [26] J. Hu and N. C. Beaulieu, "Performance analysis of decode-and-forward relaying with selection combining," *IEEE Commun. Lett.*, vol. 11, no. 6, pp. 489–491, Jun. 2007.
- [27] Z. Yang, M. Chen, W. Saad, W. Xu, M. Shikh-Bahaei, H. V. Poor, and S. Cui, "Energy-efficient wireless communications with distributed reconfigurable intelligent surfaces," *IEEE Trans. Wireless Commun.*, vol. 21, no. 1, pp. 665–679, Jul. 2021.
- [28] T. Fang and Y. Mao, "A low-complexity beamforming design for beyond-diagonal RIS aided multi-user networks," *IEEE Commun. Lett.*, vol. 28, no. 1, pp. 203–207, 2024.
- [29] C. Oestges and B. Clerckx, *MIMO wireless communications: from real-world propagation to space-time code design*. Academic Press, 2010.
- [30] X. Mu, Y. Liu, L. Guo, J. Lin, and R. Schober, "Simultaneously transmitting and reflecting (STAR) RIS aided wireless communications," *IEEE Trans. Wireless Commun.*, vol. 21, no. 5, pp. 3083–3098, Oct. 2021.